

管程转子组合式强化传热装置工业试验研究

杨卫民¹, 李锋祥¹, 陈胜利², 阎 华¹

(1. 北京化工大学 机电工程学院, 北京 100029; 2. 西安热工研究院有限公司, 陕西 西安 710032)

摘 要:介绍了当前节能降耗的迫切需要和转子组合式强化传热装置——“洁能芯”的技术原理。论述了 2 号机组甲、乙侧凝汽器性能试验内容, 试验方法和试验计算结果, 计算分析了安装转子组合式强化传热装置后凝汽器性能及机组经济性。安装转子组合式强化传热装置后, 凝汽器端差降低 2.79 °C, 真空提高 2.97 kPa, 冷却水流量减小 9.8%; 凝汽器在相同进水温度、相同真空下, 机组带负荷能力提高 19.7%; 凝汽器水阻增加 19.52 kPa。工业试验和计算分析结果表明, 转子组合式强化传热装置应用于电厂凝汽器可提高其性能。

关 键 词: 转子组合式; 强化传热; 工业试验; 汽轮发电机组

中图分类号: TK263.6 文献标识码: A

引 言

随着现代工业的飞速发展, 能源紧张的状况愈演愈烈, 世界各国都在积极寻求新能源及节能的新途径^[1]。国家发展和改革委员会发布的节能中长期专项规划指出^[2]: 我国能源效率比国际先进水平低 10 个百分点, 并且特别说明火电机组平均效率 33.8%, 比国际先进水平低 6~7 个百分点。我国能源利用率与国外有明显的差距, 节能潜力巨大, 若要达到 2010 年达到消耗标准煤 360 g/(kWh) 的标准必须依靠节能新技术。在热力发电机组中, 凝汽器是汽轮机的重要附属设备, 而其运行过程中存在的冷凝效率低下问题, 成为企业经济效益提高的瓶颈。凝汽器传热管内壁产生污垢增加了热阻, 直接影响传热效率, 引起流道变窄, 流动阻力加大, 导致动力消耗增加。而且还会由于污垢的存在而产生垢下腐蚀, 缩短设备使用寿命, 甚至导致传热管泄漏、穿孔等安全隐患。文献[3]介绍在汽轮机进汽参数和蒸汽流量不变的情况下, 凝汽器压力每降低 1 kPa, 汽轮机功率平均增加 0.7%~1%; 水冷设备换热器中水垢厚度为 2.16 mm 时, 传热系数平均下降 54%, 设备运行效率下降 50%。

针对换热器运行过程中存在的结垢问题和强化传热的需要, 许多有源强化技术和无源强化技术得到了发展和应用。螺旋扭带、螺旋弹簧、螺旋线、微型液轮机和静态混合器等管内扰流技术得到了不同程度的研究和应用^[4]。北京化工大学和北京安发电力科技有限公司联合研制的转子组合式强化传热装置——“洁能芯”, 属于管内扰流无源强化技术, 并已取得了专利保护。该装置适用于量大面广的管壳式换热器, 但目前还没有针对大型机组小管径 U 型管的解决方案。

1 转子组合式强化传热装置技术原理^[5]

1.1 强化传热机理

管内插件通过改变传热管介质流动状态以提高换热效果, 其机理是: (1) 形成旋转流, 延长水流在单位长度里通过的时间; (2) 破坏边界层; (3) 中心流体与管壁流体产生置换作用; (4) 产生二次流等^[9]。高翔等人对非衰减性旋流和衰减性旋流进行了研究^[7], 结果表明在传热系数上非衰减性旋流比衰减性旋流提高了 49%。在传热管内安装“洁能芯”后, 转子在流动介质的冲击下旋转, 流体同时也发生相应的旋转, 流体的旋转流动与转子的旋转运动满足动量矩定理。流体的旋转运动产生离心力, 导致靠近中心的流体与靠近管壁的流体发生置换, 并产生局部漩涡、二次流等。管内整体流动湍动程度增加, 层流底层变薄, 流场为以非衰减性旋转流动为主的复杂运动。且层流底层的流体随流体的整体旋转运动产生周向速度分量。层流底层的变薄和周向速度分量的产生为管内对流换热系数的提高做出了重要的贡献。这种整体的非衰减性旋转流动和局部的漩涡、二次流等脉动量有利于改善传热管介质流场的内部热交换, 从而可以大大提高管内对流换热系数。转子装置如图 1 所示。

收稿日期: 2007-07-27; 修订日期: 2007-10-25

作者简介: 杨卫民(1965—), 男, 湖南会同人, 北京化工大学教授。

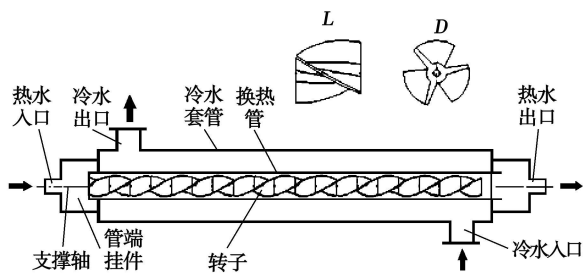


图1 转子组合式强化传热与自清洁装置

在传热管长度均为 2 000 mm 的情况下,安装“洁能芯”与光管冷却相同的水量,在相同的时间内,热水最终温度相差 3~4 °C,并且“洁能芯”起转时传热效率提高幅度最大。在电力行业,125 MW 发电机组凝汽器的端差降低 5 °C,将使得热耗降低 95.12 kJ/(kWh),煤耗减少 3.66 kg/(kWh)。由此可见,该装置能够起到良好的强化传热作用,可节能降耗,具有优良的社会经济效益。

1.2 自清洁原理

结垢是指与不洁净流体相接触而在固体表面上逐渐积聚起来的那层固态物质。根据结垢层沉积的机理,可将污垢分为颗粒污垢、结晶污垢、化学反应污垢、腐蚀污垢、生物污垢和凝固污垢。凝汽器传热管内壁污垢一般为水垢及生物粘泥,是凝汽器真空度降低的重要原因之一。结垢是一个复杂的物理化学过程,其形成过程是污垢沉积速率与剥离速率共同作用的结果^[8]。从污垢形成的机理可以看出,流体湍流程度的增加将增大对污垢层的剪切作用力,这样即可明显增加污垢的剥离速率。转子在传热管内迅速转动对管壁的污垢有 4 种作用:(1)螺棱对污垢的扫掠作用;(2)介质通过螺棱与管壁之间的间隙时高速流对管壁的冲刷作用;(3)水流通过转子时产生的离心力作用于管内壁,冲击内壁上的污垢,继而通过水流冲刷使其导出;(4)转子螺棱对沉积物的推动作用。转子的结构特点与材料特性为传热设备的安全运行提供了双重保障。同时,转子旋转引起管内的流动状态变化,使得层流底层变薄并具有了周向速度分量,这将有效破坏换热管内表面污垢沉积的物理条件。从而,“洁能芯”转子具有优异的防垢除垢功能。

2 工业试验

调停时间,在 2 号机组的乙侧凝汽器安装了转子组合式强化传热装置,甲侧凝汽器未安装。安装强化传热装置前,对甲、乙凝汽器冷却管水侧均进行了清理及高压水清洗,以使甲、乙凝汽器水侧清洁度相同。为了计算分析凝汽器转子式强化传热与自清洁装置的性能及效果,委托西安热工研究院有限公司对大唐佳木斯第二发电厂 2 号机组凝汽器进行性能试验。试验于 2007 年 4 月 25 日开始,4 月 27 日完成,共进行了如下 8 个试验工况:机组负荷 40 MW 以上,真空系统严密性试验;机组额定负荷 50 MW,甲、乙两侧凝汽器性能试验;机组负荷 40 MW 时,甲、乙两侧凝汽器性能试验;机组负荷 30 MW 时,甲、乙两侧凝汽器性能试验;机组负荷 40 MW 时,甲侧凝汽器单侧运行性能试验;机组负荷 40 MW 时,乙侧凝汽器单侧运行性能试验;机组负荷 47 MW 时,乙侧凝汽器单侧运行性能试验;机组负荷 48 MW 时,乙侧凝汽器单侧运行性能试验。

2.1 试验条件与试验相关计算

两台循环水泵运行,甲泵供甲侧凝汽器、乙泵供乙侧凝汽器;甲、乙两侧凝汽器冷却水独立运行,互相之间隔离,与临机之间隔离;机组各参数保持稳定运行;试验期间不向凝汽器补水;试验期间不得进行与试验无关的操作;试验期间发生异常情况,按照运行规程操作;每个试验工况,必须满足试验条件,稳定运行不少于 60 min,并记录数据;数据采集系统,数据记录间隔 30 s;人工数据记录间隔 2 min。

试验相关计算依据相关标准《凝汽器性能试验规程》B/T3344-93 和《表面式凝汽器》美国传热学会标准(1978)进行。温差采用对数平均温差,如式(1)所示。凝汽器热负荷以换热管内换热量为基准,如式(2)所示。传热计算按照常规的传热学计算公式进行,如式(3)所示。实验室强化传热实验往往在相同的雷诺数条件下,对强化传热性能进行比较,而本工业试验研究采用工程中常用的基于相同流速的性能比较,如式(4)和式(5)所示,参见《凝汽器性能试验规程》B/T3344-93。

2.1.1 对数平均温差 θ_{mT}

$$\theta_{mT} = \frac{\theta_{1T} - \theta_{2T}}{\ln \left(\frac{\theta_{1T}}{\theta_{2T}} \right)} = \frac{(t_{sT} - t_{1T}) - (t_{sT} - t_{2T})}{\ln \left(\frac{t_{sT} - t_{1T}}{t_{sT} - t_{2T}} \right)} = \frac{t_{2T} - t_{1T}}{\ln \left(\frac{t_{sT} - t_{1T}}{t_{sT} - t_{2T}} \right)} \quad (1)$$

式中: θ_{mT} —对数平均温差, °C; θ_{1T} —初始温差, $\theta_{1T} = t_{sT} - t_{1T}$, °C; θ_{2T} —终端温差, $\theta_{2T} = t_{sT} - t_{2T}$, °C; t_{sT} —

凝汽器压力对应的饱和温度, $^{\circ}\text{C}$; t_{2T} —凝汽器循环水的出口温度, $^{\circ}\text{C}$; t_{1T} —凝汽器循环水的进口温度, $^{\circ}\text{C}$ 。

2.1.2 凝汽器热负荷 Q_T

$$Q_T = G_{wT} \cdot C_{PT} \cdot (t_{2T} - t_{1T}) \quad (2)$$

式中: Q_T —凝汽器试验热负荷, kW; G_{wT} —试验循环水流量, kg/s; C_{PT} —试验循环水的平均温度下的比热容, kJ/(kg $\cdot^{\circ}\text{C}$)。

2.1.3 凝汽器总体传热系数 K_T

$$K_T = \frac{Q_T}{A \times \theta_{mT}} = \frac{G_{wT} \cdot C_{PT} \cdot 10^3}{A \times (t_{2T} - t_{1T})} \times \ln \left[\frac{\theta_{1T}}{\theta_{2T}} \right] \quad (3)$$

式中: K_T —试验凝汽器总体传热系数, W/(m $^2\cdot^{\circ}\text{C}$); A —凝汽器换热面积, m 2 。

2.1.4 冷却水流量对试验传热系数 K_T 的修正系数 F_v

$$K_C = K_T F_v \quad (4)$$

$$F_v = \sqrt{v_D / v_T} \quad (5)$$

式中: K_C —修正后的总体传热系数; F_v —流量修正系数; v_T —试验时冷却管内平均流速, m/s; v_D —修正后冷却管内平均流速, m/s。

2.2 甲、乙两侧凝汽器同时运行性能试验

在进行凝汽器的真空系统严密性试验后, 在保证系统严密性的情况下, 进行凝汽器性能试验。

试验期间两台循环水泵运行, 甲、乙两侧凝汽器同时运行, 甲泵供甲侧凝汽器、乙泵供乙侧凝汽器。试验时, 关闭 1 号和 2 号机组循环水 2 个联络门; 关闭 2 号机组甲、乙两侧凝汽器循环冷却水联络门; 使甲、乙两侧凝汽器冷却水独立运行, 互相之间隔离, 与临机之间隔离。试验期间, 主蒸汽压力、主蒸汽温度和机组负荷保持稳定运行。凝汽器性能试验进行了 50、40 和 30 MW 负荷工况, 对甲、乙凝汽器运行数据分别进行了测量, 并分析试验数据及计算结果。

2.2.1 机组功率 49.66 MW, 凝汽器压力 5.15 kPa, 50 MW 负荷工况

(1) 甲侧凝汽器(未装转子组合式强化传热装置)冷却水量 4 215.86 m 3 /h, 传热端差 10.73 $^{\circ}\text{C}$, 温升 16.70 $^{\circ}\text{C}$, 热负荷 294 717.61 MJ/h, 总体传热系数 2.63 kW/(m $^2\cdot^{\circ}\text{C}$);

(2) 乙侧凝汽器(安装转子组合式强化传热装置)冷却水量 3 468.50 m 3 /h, 传热端差 11.82 $^{\circ}\text{C}$, 温升 15.61 $^{\circ}\text{C}$, 热负荷 226 685.83 MJ/h, 总体传热系数 1.94 kW/(m $^2\cdot^{\circ}\text{C}$);

(3) 甲、乙两侧凝汽器冷却水量都修正到乙侧凝汽器冷却水量 3 468.50 m 3 /h 后, 乙侧凝汽器真空比甲侧高 1.29 kPa。

2.2.2 机组功率 40.64 MW, 凝汽器压力 4.58 kPa, 40 MW 负荷工况

(1) 甲侧凝汽器(未装转子组合式强化传热装置)冷却水量 4 164.47 m 3 /h, 传热端差 11.07 $^{\circ}\text{C}$, 温升 14.04 $^{\circ}\text{C}$, 热负荷 244 921.18 MJ/h, 总体传热系数 2.27 kW/(m $^2\cdot^{\circ}\text{C}$);

(2) 乙侧凝汽器(安装转子组合式强化传热装置)冷却水量 3 419.77 m 3 /h, 传热端差 11.91 $^{\circ}\text{C}$, 温升 13.20 $^{\circ}\text{C}$, 热负荷 189 100.16 MJ/h, 总体传热系数 1.70 kW/(m $^2\cdot^{\circ}\text{C}$);

(3) 甲、乙两侧凝汽器冷却水量都修正到乙侧凝汽器冷却水量 3 419.77 m 3 /h 后, 乙侧凝汽器真空比甲侧高 1.03 kPa。

2.2.3 机组功率 30.90 MW, 凝汽器压力 4.10 kPa, 30 MW 负荷工况

(1) 甲侧凝汽器(未装转子组合式强化传热装置)冷却水量 4 155.148 m 3 /h, 传热端差 11.97 $^{\circ}\text{C}$, 温升 11.14 $^{\circ}\text{C}$, 热负荷 194 036.57 MJ/h, 总体传热系数 1.82 kW/(m $^2\cdot^{\circ}\text{C}$);

(2) 乙侧凝汽器(安装转子组合式强化传热装置)冷却水量 3 378.68 m 3 /h, 传热端差 13.18 $^{\circ}\text{C}$, 温升 9.93 $^{\circ}\text{C}$, 热负荷 140 647.84 MJ/h, 总体传热系数 1.26 kW/(m $^2\cdot^{\circ}\text{C}$);

(3) 甲、乙两侧凝汽器冷却水量都修正到乙侧凝汽器冷却水量 3 378.68 m 3 /h 后, 乙侧凝汽器真空比甲侧高 0.86 kPa。

以上 3 个负荷工况, 由于甲、乙两侧凝汽器同时运行, 无法区分甲、乙两侧凝汽器汽侧的运行状况, 不能完全确定强化传热装置的运行效果。凝汽器的运行性能是甲、乙两侧凝汽器运行的综合效果。

2.3 甲、乙两侧凝汽器单侧运行带负荷能力性能试验

试验期间单侧凝汽器、单台循环水泵运行, 甲泵供甲侧凝汽器、乙泵供乙侧凝汽器。试验时, 关闭 1 号和 2 号机组循环水 2 个联络门; 关闭 2 号机组甲、乙两侧凝汽器循环冷却水联络门。试验期间, 主蒸汽压力、主蒸汽温度和机组负荷保持稳定运行。甲侧凝汽器单侧运行性能试验进行了 40 MW 负荷工况, 乙侧凝汽器单侧运行性能试验进行了 40、47 和 48 MW 3 个负荷工况。

2.3.1 甲侧凝汽器 40 MW 单侧运行

机组功率 40.36 MW, 凝汽器压力 14.92 kPa, 冷却水进水温度 3.94 $^{\circ}\text{C}$, 冷却水流量 4 725.94 m 3 /h, 冷却水温升 29.08 $^{\circ}\text{C}$, 端差 20.86 $^{\circ}\text{C}$, 热负荷 574 320.97 MJ/h。

2.3.2 乙侧凝汽器 40 MW 单侧运行

机组功率 40.44 MW, 凝汽器压力 12.02 kPa, 冷却水进水温度 5.55 °C, 冷却水流量 4 262.66 m³/h, 冷却水温升 25.87 °C, 端差 18.07 °C, 热负荷 460 702.54 MJ/h。

将冷却水进水温度修正到甲侧进水温度 3.94 °C, 则凝汽器压力 11.95 kPa。

2.3.3 在 40 MW 负荷下, 甲乙凝汽器单侧运行比较

乙侧凝汽器进水温度比甲侧高 1.61 °C, 冷却水流量比甲侧小 9.8% (小 463.27 m³/h), 端差比甲侧低 2.79 °C, 汽轮机低压缸排汽压力比甲侧运行时低 2.9 kPa。如果乙侧凝汽器进水温度与甲侧相同, 则乙侧凝汽器压力 11.95 kPa, 比甲侧运行时低 2.97 kPa。

2.3.4 乙侧凝汽器 47 MW 单侧运行

机组功率 47.0 MW, 凝汽器压力 14.57 kPa, 冷却水进水温度 6.07 °C, 冷却水流量 4 196.07 m³/h, 冷却水温升 29.74 °C, 端差 17.58 °C, 热负荷 520 974.70 MJ/h。

将冷却水进水温度修正到甲侧进水温度 3.94 °C, 则凝汽器压力 14.47 kPa。

2.3.5 乙侧凝汽器 48 MW 单侧运行

机组功率 48.31 MW, 凝汽器压力 15.38 kPa, 冷却水进水温度 7.00 °C, 冷却水流量 4 183.35 m³/h, 冷却水温升 30.11 °C, 端差 17.41 °C, 热负荷 525 621.04 MJ/h。

将冷却水进水温度修正到甲侧进水温度 3.94 °C, 则凝汽器压力 15.20 kPa。

2.3.6 单侧运行试验结果分析结论

(1) 机组相同负荷下, 安装转子组合式强化传热装置的乙侧凝汽器比未安装的甲侧真空提高 2.97 kPa;

(2) 乙侧凝汽器冷却水流量比甲侧小 9.8%;

(3) 甲、乙两侧凝汽器在相同真空下 (约 15 kPa), 安装转子组合式强化传热装置的乙侧凝汽器带负荷 48.31 MW, 未安装转子组合式强化传热装置的甲侧凝汽器带负荷 40.36 MW, 乙侧比甲侧多带负荷 7.95 MW, 多 19.7%。

2.4 阻力试验

凝汽器冷却管内安装转子组合式强化传热装置后, 凝汽器的水阻增加, 循环水泵扬程增加, 冷却水流量减小。由于 2 号机组凝汽器进水压力测点在进水垂直管段上, 出水压力测点在出水室顶部, 所以测

量的凝汽器阻力没有完全包含出水室的阻力。甲、乙两侧凝汽器的阻力对比如表 1 所示。根据试验结果, 安装装置后, 使凝汽器水阻增加了 19.52 kPa, 凝汽器阻力系数增加了 23.28。

表 1 甲、乙两侧凝汽器阻力对比

	甲(无转子)	乙(有转子)
凝汽器冷却水量/m ³ ·h ⁻¹	4 215.86	3 468.50
冷却管内流速/m ² ·s ⁻¹	1.80	1.48
凝汽器水阻/m	1.87	3.86
阻力系数	11.37	34.65
水阻比甲侧大/m	0	1.99
阻力系数比甲侧大	0	23.28

3 结 论

大唐佳木斯第二发电厂 2 号汽轮发电机组凝汽器乙侧安装转子组合式强化传热装置后, 效果显著, 经济效益明显。安装转子组合式强化传热装置后, 凝汽器端差降低 2.79 °C, 真空提高 2.97 kPa; 冷却水流量减小 9.8%; 凝汽器在相同进水温度和相同真空下, 安装转子组合式强化传热装置后比安装前机组多带负荷 19.7%; 安装转子组合式强化传热装置后, 凝汽器水阻增加了 19.52 kPa, 在工程许可范围之内。

参考文献:

- [1] 崔海亭, 彭培英. 强化传热新技术及其应用[M]. 北京: 化学工业出版社, 2006.
- [2] 国家发展和改革委员会. 节能中长期专项规划[J]. 节能与环保, 2004(11): 3-10.
- [3] 《中国电力百科全书》编辑委员会. 中国电力百科全书[M]. 北京: 中国电力出版社, 2001.
- [4] BERGLIES ARTHUR E. ExHFT for fourth generation heat transfer technology[J]. Experimental Thermal and Fluid Science, 2002 26: 335-344.
- [5] 杨卫民. 洁能芯节能原理及应用[J]. 化工进展, 2006, 25(增刊): 198-200.
- [6] 洪蒙纳, 邓先和. 管壳式换热器管程强化传热研究进展[J]. 广东化工, 2005(3): 41-42.
- [7] 高翔. 螺旋肋片形成非衰减性旋流的强化传热性能[J]. 化工学报, 2003, 54(9): 1205-1208.
- [8] 杨善让, 孙灵芳, 徐志明. 换热设备污垢研究的现状和展望[J]. 化工进展, 2004 23(10): 1091-1098.

(编辑 单丽华)

甲醇/电联产系统中甲醇合成与精馏模拟及变负荷研究 = **A Study of Methanol Synthesis, Distillation Simulation and Load Variation of a Methanol/Power Cogeneration System**[刊, 汉] / WANG Ming-hua, LI Zheng, FENG Jing, et al (Thermal Energy Engineering Department, Tsinghua University, Beijing, China, Post Code: 100084) // Journal of Engineering for Thermal Energy & Power. — 2008, 23(4). — 363 ~ 368

As one of the most promising clean-coal-fired power generation technologies, an integrated gasification combined cycle (IGCC) system coupled with a methanol synthesis system not only can enhance the load regulating ability of the system but also simultaneously improve the cost-effectiveness of the IGCC power plants. The flow path in the process of C301 type LP tube row gas-phase methanol synthesis and three-tower distillation was simulated through the use of software ASPEN, and a tactic for load-variation regulation based on the divided flow ratio and circulation ratio has been proposed. With the help of a four-quadrant chart, the methanol load variation range and the ability of regulating power loads under the condition of different divided flow ratios and circulating ratios were shown. In addition, a load variation regulation of distillation processes was accomplished through a change of the reboiling and condensing loads of various distillation towers. **Key words:** methanol/power cogeneration, IGCC (integrated gasification combined cycle), methanol synthesis, methanol distillation, load variation

悬臂转子远端优化主动平衡技术研究 = **A Study of the Active Balancing Technology for the Far End Optimization of a Cantilever Rotor**[刊, 汉] / SU Yi-nu, HE Li-dong, FENG Wei (Diagnosis and Self-healing Engineering Research Center, Beijing University of Chemical Technology, Beijing, China, Post Code: 100029) // Journal of Engineering for Thermal Energy & Power. — 2008, 23(4). — 369 ~ 372

To guide the application of an active balancing device in industrial cantilever rotors, a cantilever rotor test stand was set up to perform an experimental study of active balancing technology. The results of finite-element simulation calculation of a test stand rotor show that the balancing device installed on a coupling can effectively reduce the vibration caused by any imbalance of a flying wheel. At two rotating speeds, both amplitudes of 2 # bearing can be reduced by over 25%. However, during the vibration reduction of 2 # bearing, the vibration of 1 # bearing will increase rapidly. An optimized control over 1 # and 2 # bearing vibration was proposed to make the vibration of both bearings at the operating speed not exceed alarm value 50 μ m. Based on the idea of an optimized control, hydraulic automatic balancing experiments at several rotating speeds were performed on the cantilever rotor test stand. The test results verified the conclusion of the simulation calculation, and the amplitude reduction of 2 # bearing amounts to over 30%, achieving a relatively good balancing effectiveness. The numerical simulation and experimental study have laid a foundation for the application of active balancing technology to cantilever rotors in engineering practice. **Key words:** cantilever rotor, active balance, vibration, optimized control

长外伸段转子高速动平衡时支承方式的研究 = **A Study of the Supporting Modes for a Long Overhanging Rotor During a High-speed Dynamic Balancing Process**[刊, 汉] / QI Nai-bin, YUAN Qi, RAO Jin-yang (College of Energy Source and Power Engineering, Xi'an Jiaotong University, Xi'an, China, Post Code: 710049) // Journal of Engineering for Thermal Energy & Power. — 2008, 23(4). — 373 ~ 377

For large capacity steam turbines, the overhanging section of a LP rotor must be lengthened due to the restrictions of an exhaust hood structure. This may bring about a great difficulty for the shop high-speed dynamic balance of the rotor owing to the influence of the rotational inertia of the long overhanging section. To study the supporting modes for the rotor in question during the high-speed dynamic balance, set up was a test rig for a model rotor with a long overhanging section. Tests were performed respectively with the bearing points being moved outward and an auxiliary bearing being added. The test results show that for rotors with a long overhanging section, the method of adding an auxiliary bearing can effectively reduce the first order resonant amplitude of rotors at the main bearing points. Furthermore, there exists an optimum choice for the auxiliary bearing position. **Key words:** long overhanging section, rotor, high speed dynamic balance, supporting mode

管程转子组合式强化传热装置工业试验的研究 = **Commercial and Experimental Study of a Rotor-assembly Type Intensified Heat-transfer Device at the Tube Side**[刊, 汉] / YANG Wei-min, LI Feng-xiang, YAN Hua (College

of Electro-mechanical Engineering, Beijing University of Chemical Technology, Beijing, China, Post Code: 100029), CHEN Sheng-li (Xi'an Thermodynamics Academy Co. Ltd., Xi'an, China, Post Code: 710032)// Journal of Engineering for Thermal Energy & Power. — 2008, 23(4). — 378 ~ 381

Current urgent demands for energy-saving and consumption reduction were described along with the technical theory of a rotor-assembly type intensified heat-transfer device—"Clean-energy Core". The above device has been installed on the 2[#] turbo-generator unit of Datang Jiamusze No. 2 Power Plant. The condenser at one side of the turbo-generator unit was provided with the device in question while the condenser at another side of the unit was not. The performance test content, testing method and the calculation results of the two condensers of the No. 2 power plant were discussed. The performance of the two condensers and the cost-effectiveness of the No. 2 unit after installation of the device on one condenser were calculated and analyzed. After the installation of the above-cited device, the terminal temperature difference of the relevant condenser drops by 2.79 °C, its vacuum increases by 2.97 kPa and its cooling water flow rate decreases by 9.8%. Under the condition of the condensers having the same inlet water temperature and vacuum, the load bearing capacity of the turbo-generator unit will increase by 19.7%, and the water resistance of the condensers increase by 19.52 kPa. The results of the industrial experiments and analytic calculation show that the rotor-assembly type intensified heat-transfer device can be used for condensers in power plants to improve their performance. **Key words:** rotor-assembly type, intensified heat transfer, industrial experiment, turbo-generator unit

平衡目标选择与全息动平衡法的改进研究= A Study on the Improvement of Balancing Target Selection and Holographic Dynamic Balancing Method[刊, 汉] / LIAO Yu-he, LANG Gen-feng, QU Liang-sheng (Intelligent Instrument and Monitoring/diagnosis Research Institute, College of Mechanical Engineering, Xi'an Jiaotong University, Xi'an, China, Post Code: 710049)// Journal of Engineering for Thermal Energy & Power. — 2008, 23(4). — 382 ~ 386

Discussed were the problems existing during the description of the balancing state of a rotor by using a working-frequency trajectory initial-phase vector, which serves as a balancing target in a holographic dynamic-balancing method. Through a precession decomposition of the working-frequency trajectory of the rotor, the different influences of the unbalanced mass of the rotor on its positive and reverse precession component were analyzed in detail. It has been shown that the reverse precession component is not a direct reflection of the balancing state of the rotor. Under the condition of a trajectory with a large eccentricity, the interference on the estimation of the unbalanced mass caused by the reverse precession component should not be neglected. On this basis, presented was an improved holographic dynamic-balancing method with the positive-precession component trajectory initial-phase vector of the rotor serving as a balancing target. Under the condition of not influencing the balancing accuracy of the original holographic dynamic-balancing method, the counterweight version calculation process has been simplified. Compared with the traditional balancing methods, the method under discussion is more accurate and effective. On-site practical applications have verified the reliability and validity of the method. **Key words:** rotor, holographic dynamic-balancing, precession, initial phase vector

大颗粒振动流化床与水平管平均传热特性研究= A Study of the Characteristics of Average Heat Transfer Between a Big-particle Dominated Vibrating Fluidized Bed and Horizontal Tubes[刊, 汉] / ZHU Xue-jun, YE Shi-chao, SHI Jin-xia, et al (College of Chemical Engineering, Sichuan University, Chengdu, China, Post Code: 610065)// Journal of Engineering for Thermal Energy & Power. — 2008, 23(4). — 387 ~ 390

In a two-dimensional fluidized bed (240 mm × 80 mm), with glass beads of average diameters d_p of 0.71 mm and 1.83 mm and millet of 1.66 mm diameter serving as materials, studied was the heat transfer law between the vibrating fluidized bed and submerged horizontal tubes. The influence of such factors as gas flow speed, vibration frequency, bed height and diameters of horizontal tubes etc. on the average heat transfer coefficient was investigated. The results of the study show that with an increase of the vibration frequency, the optimum gas flow speed will decrease, and with an increase of the gas flow speed, the optimum vibration frequency will also go down. The average heat transfer coefficient will increase with a decrease of the particle diameter. The particle thermo-physical properties and the tube diameter also have a relatively big influence on the average heat transfer coefficient. From the test data, a correlation formula for the calculation of the average heat transfer coefficient has been obtained. The calculation values have been in relatively good agreement with the test ones, and the calculation error is within a range of $\pm 10\%$. The above results can serve as reference data for the design and study of vibrating fluidized beds fitted with submerged horizontal tubes. **Key words:** vibrating fluidized bed, average